How do thermal optimisations on the CCS charging inlet affect the charging time?

Dipl.-Ing. Jochen Krings, Daimler Truck AG
Department: Charging Components E-Mobility DTB
jochen.krings@daimlertruck.com

Daimler Truck AG
Fasanenweg 10
70771 Leinfelden-Echterdingen, Germany

Prof. Dr.-Ing. Hans-Christian Reuss, Universität Stuttgart / FKFS Stuttgart
Head of Board of Management for Vehicle Mechatronics
info@fkfs.de

FKFS (Forschungsinstitut für Kraftfahrwesen und Fahrzeugmotoren) Stuttgart
Pfaffenwaldring 12
70569 Stuttgart, Germany

Dipl.-Ing. Peter Ziegler, Daimler Truck AG
Department Leadership: Charging Components E-Mobility DTB
peter.z.ziegler@daimlertruck.com

B. Eng. Paul Steinmetz, Daimler Truck AG
Department: Charging Components E-Mobility DTB
paul.ps.steinmetz@daimlertruck.com

Daimler Truck AG
Fasanenweg 10
70771 Leinfelden-Echterdingen, Germany

Contribution: 2025 FKFS Conference on Vehicle Aerodynamics and Thermal Management
15 – 16 October 2025 | Leinfelden-Echterdingen

Abstract:

The CCS charging standard is the most widely used variant for charging electric vehicles in Europe. The further development of the charging components enables charging capacities to be achieved that reach the limits of the CCS standard. One way to increase the effective charging power is to reduce charging losses.

In this work, one approach to optimising the CCS charging inlet is presented using a specially developed thermal Matlab/Simscape simulation. Comparisons of the thermal results from the current CCS inlet and the version with optimisation approach show slower heating. This offers the possibility of charging with a higher current over a longer period of time before the permissible limit temperature is reached.

In addition, the time saving potential due to the increased charging performance of the CCS charging inlet is analysed and the reduction in charging time is derived.

Figure 1: left: Mercedes Benz eActros 600
right: detail view CCS inlet with charing gun
copyright: Daimler Truck AG

1 Introduction

In the course of the global electrification of the automotive sector, commercial vehicles with electric drives have also been increasingly developed in recent years [1].

Compared to cars for private transport, fast charging of large energy storage units is a major challenge in the commercial vehicle sector in particular [2]. A short downtime thanks to fast charging times enables faster availability of commercial vehicles. This is of great importance for the economic efficiency of logistics operations [3].

Due to the widespread use of CCS (Combined Charging System) throughout Europe, electrified commercial vehicles also use this charging standard.

Fast charging of the energy storage units via the CCS charging inlet requires correspondingly high charging capacities, which are accompanied by high charging currents. The commercial vehicle sector is pushing itself to the limits of the CCS standard [4].

Accompanied by charging currents of several hundred amps and the electrical resistance of the charging components, there are also losses in the form of heat. In order to increase charging efficiency, it is always desirable to keep the overall heat development as low as possible. In addition to saving energy costs, the cooling components can also be smaller on the vehicle side, which results in a lighter vehicle weight and thus lower energy consumption when driving [5].

At the same time, a lower and slower temperature rise in the charging components also leads to lower material stress due to temperature differences, which promotes the longevity of the charging components [6].

The aim when designing the charging path components is always to maintain the maximum permissible charging current for as long as possible and not to exceed the temperature limit value of touchable components in order to protect people.

Thermal simulation tests are suitable for checking thermal optimisation approaches at an early stage in charging component development. The simulation-based testing of the new design approaches for component optimisation allows the expected results to be quantified in advance and, in the best case, iteration loops in component development to be reduced.

In the following, a thermal optimisation approach of the CCS charging inlet is tested by means of software simulation and the results are presented.

2 Design of the CCS charging inlet

The design of a CCS charging inlet is shown in Figure 2.

Coming from the charging station via the charging gun, the current is led via the contact pins into the inside of the charging inlet to the connection plates. These are connected to the bus bars for the cable via a screw connection. The temperature is monitored separately for positive and negative via sensors located between the contact pins and the connection plates. The maximum temperature is 90°C, according to DIN EN IEC 62196-1, [7].

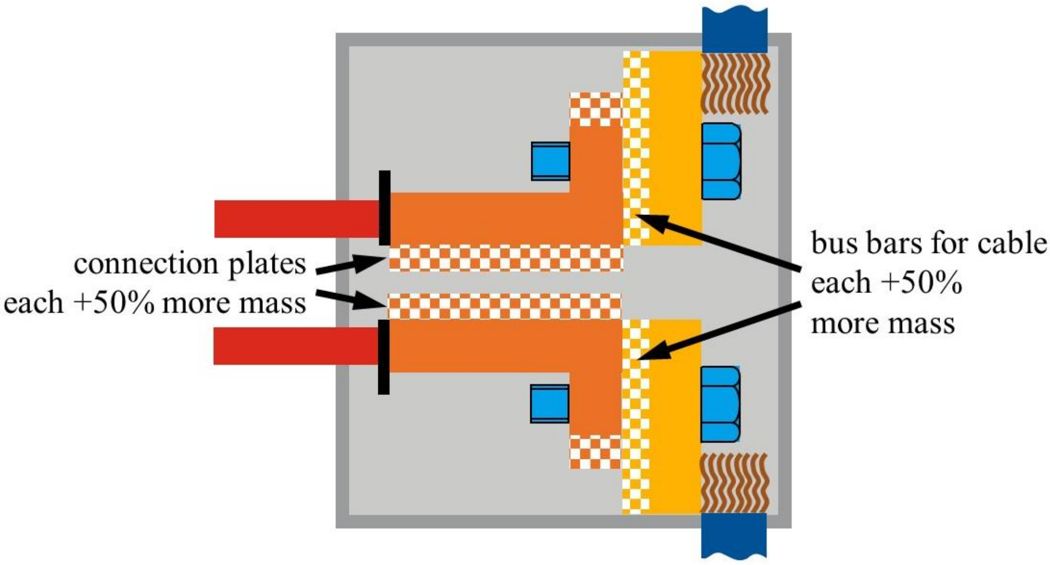

Figure 2: Schematic of internal design of CCS charging inlet
copyright: Daimler Truck AG

3 Modelling and simulation setup

Due to the electrical resistance of current-carrying components, internal losses occur, which lead to heating [8]. By means of Ohm's law Eq. (1), the electrical power Eq. (2) can be described with the voltage U, the current I and the electrical resistance $R_{electrical}$. Analogous to the electrical power, Joule's heating $P_{thermal}$, or the resulting heat flow $\dot{Q}$, can be described by Eq. (3):

Ohm's Law: $$U = I * R_{electrical} \quad (1)$$

Electrical Power: $$P_{electrical} = I * U = I^2 * R_{electrical} \quad (2)$$

Joule's Heathing: $$P_{thermal} = \dot{Q} = I^2 * R_{thermal} \quad (3)$$

The thermal resistance $R_{thermal}$ is described in Eq. (4) [9] by the length l of the component, the thermal conductivity λ as a material property and the component cross-sectional area A:

Thermal resistance: $$R_{thermal} = \frac{l}{\lambda * A} \quad (4)$$

Based on the "Technical Guideline for Thermosimulation Models" of the ZVEI (Zentralverband Elektrotechnik- und Elektroindustrie) the coupling of electrothermal simulations can be illustrated as follows [10]:

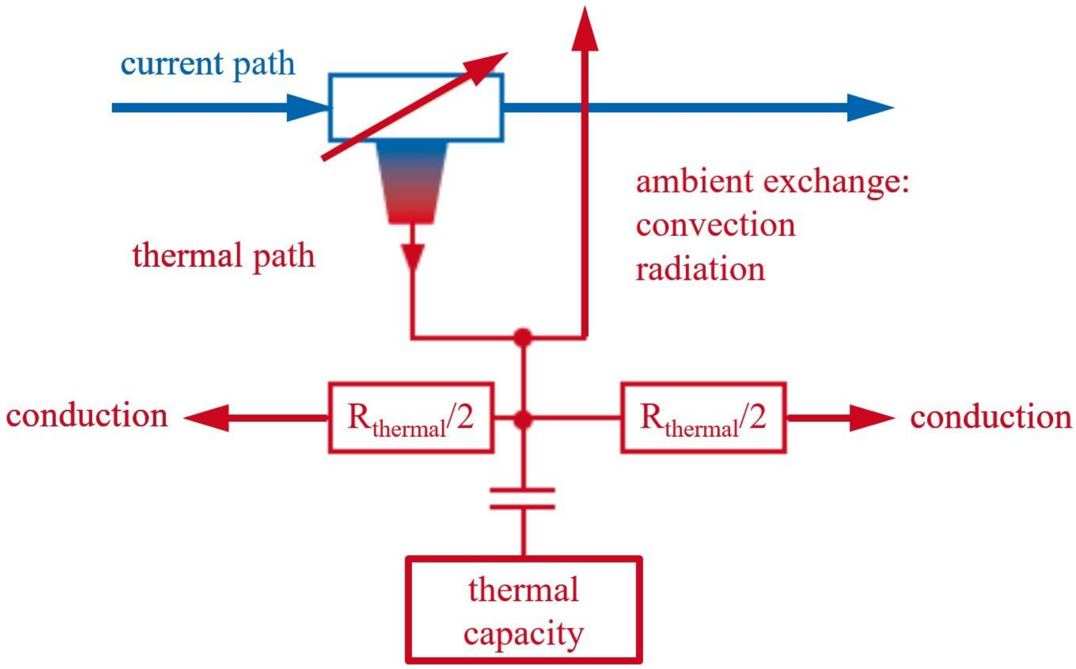

Figure 3: ZVEI Guideline Schematic for Electro-Thermal Coupling
copyright: ZVEI

An electrical component with its heat production is interpreted as a thermal source. Part of the heat can be absorbed by the component itself, which is called thermal capacity. Furthermore, heat can, for example, be exchanged with the ambient air by convection or radiated by radiation [11].

The heat conduction of the component is referred to as conduction. Since the heat input in the middle of the component is assumed in the modelling, the thermal resistance of the conduction is distributed in half in both directions.

For the structure of the thermal simulation in Matlab/Simscape, all current-carrying components can be represented as a series connection of electrical and thermal resistors, as shown in Figure 3. The components interact with each other through conduction, convection and radiation.

4 Design improvement potential: Increase in thermal mass connection

The conflicting goal of rapid charging of the energy storage unit results in increased heat development at high currents, which increases with the second power, see Eq. (3). One way to delay reaching the limiting temperature is to increase the thermal capacity C_{th} of the connection plate and the bus bar of the cable. The thermal capacity C_{th} describes the ability of a body to store and release thermal energy. It is proportional to the material property of the specific heat capacity c and the mass m of the component, see Eq. (5), [11]:

$$C_{th} = m * c \tag{5}$$

Multiplying the thermal capacity C_{th} with the temperature change dT as a derivation after the time dt, results in the heat flow $\dot{Q}$ that the body absorbs or emits, see Eq. (6), [12]:

$$\dot{Q} = C_{th} * \frac{dT}{dt} = m * c * \frac{dT}{dt} \tag{6}$$

The mass of the live parts can be easily increased by the material thickness and requires only minor adjustments in the given installation space without affecting the outer contour of the housing.

In addition to absorbing energy in the form of heat, the current-carrying parts can also transfer the heat within the component or to other components. This effect is called conduction. The heat flow $\dot{Q}_{conduction}$ can be determined with the thermal resistance $R_{thermal}$ Eq. (4) and the temperature difference ΔT, Eq. (7), [12]:

$$\dot{Q}_{conduction} = \frac{1}{R_{thermal}} * \Delta T = \frac{\lambda * A}{l} * \Delta T \tag{7}$$

The increase in the material thickness of the current-carrying parts results in a proportional increase in the cross-section A. This also results in a greater heat flow through conduction, which promotes the removal of heat.

5 Simulation-based test: increase in thermal mass

For the simulation-based test, the material thickness of the connection plates and the bus bars of the cables are increased by a factor of 1.5. This also increases the mass and the component cross-section by a factor of 1.5. In absolute terms, the mass of the components only increases by a few grammes. The temperature heating of the current design as the basis is compared with the results from the simulation for the variant with the increased thermal mass.

A start and ambient temperature of 25°C are assumed as boundary conditions. With a sufficient distance to the maximum permissible temperature of 90°C, an end temperature of 85°C is specified at the contact pins.

The charging current is initially constant 500A and is reduced after reaching 85°C until a constant temperature value is set at the contact pin.

The set cooling value per contact pin is 3.5W and is discharged via the charging station's charging gun [13].

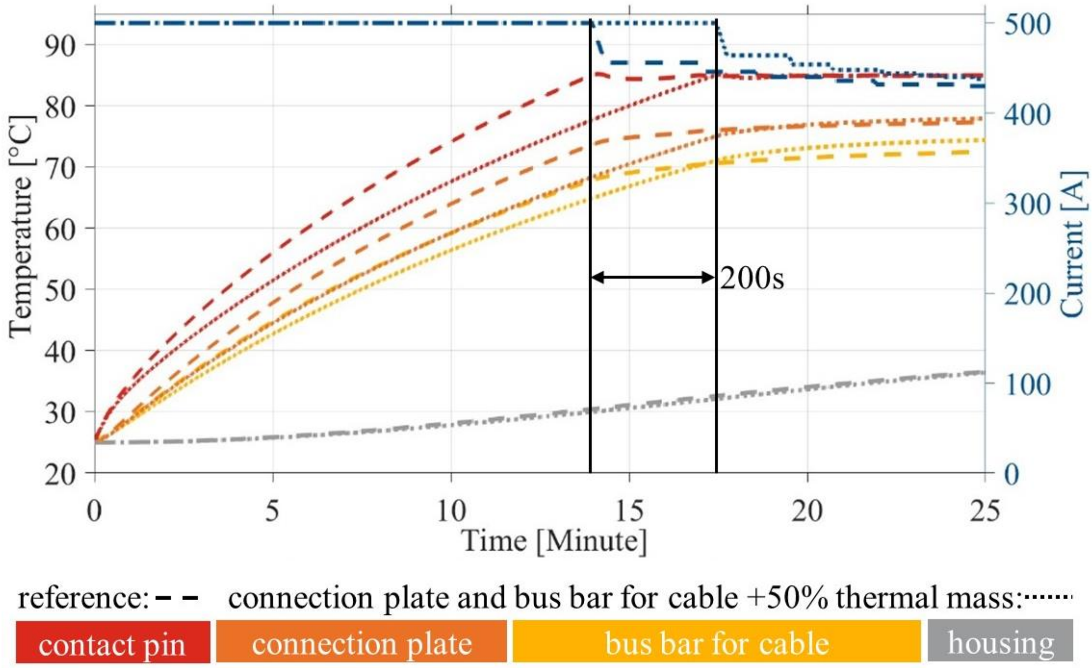

Figure 4: Comparison of basic version with adaptation of connection plate and bus bar of the cables with 1.5x thermal mass
copyright: Daimler Truck AG

6 Evaluation of the simulation test results

The start-up and ambient temperature is 25°C for both the basic version and the adapted version. With a constant charging current of 500A, blue graphs, the contact pin of the basic version, red dashed graph, reaches the final temperature of 85°C defined for the simulation within 837s. In the adapted version, the red dotted graph, the final temperature of 85°C is not reached until 209 seconds later. This means that the charging time at 500A can be maintained by 25% longer.

This is due to the increased thermal mass from the connection plate and bus bar of the cable. According to Eq. (5), the thermal capacity is increased by increasing the masses, which enables a higher heat flow $\dot{Q}$ Eq. (6) and thus serves as a larger heat sink. Due to the ability to absorb more heat, both the connecting plate, orange graph, and the bus bars of the cable, yellow graph, heat up more slowly. The reduction of the thermal resistance $R_{thermal}$ also increases the conductive heat flow $\dot{Q}_{conduction}$ Eq. (7). This allows the heat to be dissipated more quickly to adjacent components and the housing, grey graphs.

To counteract exceeding the end temperature, the charging current must be reduced after reaching a temperature at the contact pin of 85°C. In the basic version, the charging current is initially reduced to 456A for 170s until a constant temperature of 85°C is reached at the contact pin after a further reduction to 440A after 103s. In the adapted version, the charging current is initially reduced to 464A for 123s. After the subsequent reduction to 448A after 71s, a constant temperature of 85°C is also set at the contact pin. This means that the continuous charging current is 8A higher than in the basic version. Overall, this results in a greater amount of electrical energy being introduced into the system compared to the basic version. This is equivalent to a higher heat flow according to Eq. (3). The result can be seen in the two graphs of the connection plate, orange, and the busbar for the cable, yellow. Both dotted lines are above the temperature level of the respective basic version, shown in dashed lines. A similar process can also be seen in the heating of the housing, grey lines, even if the temperature difference is only slightly pronounced. The increased electrical energy input is also reflected here in the increased waste heat at a higher housing temperature. As the mass and conductive surface of the housing is large compared to the live parts, the small temperature differences can be explained.

7 Energy consumption CCS charging inlet

The simulation model of the CCS charging inlet is examined for the energy balance calculation. The amount of heat generated during the charging process in the initial situation serves as a reference value for comparing the optimisation approach of the CCS charging inlet. The system limit for the calculation extends up to the plug of the high-voltage cables of the CCS charging inlet. For this purpose, the heat flow through Joule's heating is calculated as an integral over time at all current conductors.

In order to compare the different optimisation approaches, the amount of electrical energy required to increase the vehicle's energy storage from a charge level of 20% to 80% is selected. In reality, this usually corresponds to the range of electrical energy storage units in which a constant charging power can be absorbed without having to be derated due to temperature or saturation. In the special case of this simulation, this corresponds to a charged energy quantity of 360kWh. This would result in a theoretical charging time of 56 minutes with a constant charge of 500A.

The simulation of the reference model of the CCS charging inlet including the high-voltage cables generates a heat quantity of 75.8Wh during the charging process. The temperature-related reduction of the charging current results in a total charging time of 63.7 minutes in the 360kWh transmitted.

CCS inlet	produced heat		charging time	
	[Wh]	[%]	[min]	[%]
reference	75,8	-	63,7	-
increase of thermal mass +50%	77,5	2,2	62,4	-2,0

Figure 5: CCS inlet: max. 500A, 360kWh, 25°C air temperature

The optimisation approach with the increased thermal mass of the connection plates and the bus bars of the cables of the CCS charging inlet by 50% leads to a time delay until the maximum temperature at the CCS charging inlet is reached. The charging current of 500A can thus be maintained for about 200 seconds longer. The permanently transferable charging current is 10A higher than that of the reference version. The higher charging power over a longer period of time leads to an increase in the amount of heat in the CCS charging inlet to 77.5Wh and thus an increase of 2.2%. The increased amount of heat is temporarily stored in the thermal mass of the current-conducting bus bars. The charging time, on the other hand, is reduced by 2%, which corresponds to a shorter charging time of just over one minute.

8 Conclusion

The expected results could be quantified in advance by means of thermal simulation-based testing of the new design approach for increasing the thermal mass of live conductors in the CCS charging inlet.

The comparison between the reference version and the design optimisation showed slower heating due to the higher thermal capacity. As a result, the constant charging current of 500A could be maintained for 209s or 25% longer until the defined limit temperature of 85°C was reached. This result is equivalent to a larger, charged amount of energy at the same time. Since the adjustments to the current conductors mean only a few grammes more material in absolute terms despite the enlargement by a factor of 1.5, the changes are minimal overall. This design approach can therefore be implemented in the existing housing.

Due to the modular design of the thermal test simulation, it is possible to carry out further comparisons and investigations of new solution approaches for thermal optimisation of the CCS charging inlet in special or comparable components from the charging path in general.

The test simulation can thus reduce the number of iteration loops of design approaches for component optimisation and thus reduce development time and costs.

In addition to the fact that the charging current can be kept at a higher level for longer due to the optimisation approach, the charging time is also reduced. This is important with regard to fast charging in order to promote fast vehicle availability. In addition, the improvement measures also result in energy saving potential if the charging current is reduced and the maximum permissible temperature of the CCS charging inlet is not exceeded.

9 Reference list

[1] Infineon Technologies AG, Neubiberg, Germany, https://community.infineon.com/t5/Blogs/Driving-the-Future-of-Electrified-Commercial-Vehicles/ba-p/916830#., online 15.09.2025

[2] Daimler Truck AG, Leinfelden-Echterdingen, Germany, https://hub.mercedes-benz-trucks.com/de/de/trucks/eactros-600.html, online 15.09.2025

[3] S. Schulze, “Ist Megawatt Laden die Zukunft? Potentiale, Herausforderungen und Risiken”, Daimler Truck AG, tme (Lehrstuhl für Thermodynamik mobiler Energiewandlungssysteme), RWTH Aachen University, Aachen, March 2024

[4] B. Horrmeyer, DKE (Deutsche Kommission Elektrotechnik Elektronik Informationstechnik), https://www.dke.de/de/arbeitsfelder/mobility/news/megawatt-charging-system-elektrifizierung-schwerlastverkehr, online 15.09.2025

[5] R. Collin, Y. Miao, A. Yokochi, P. Enjeti, A. v. Jouanne, “Advanced Electric Vehicle Fast-Charging Technologies“, MDPI: Energies, May 2019

[6] M. Thoben, F. Sauerland, K. Mainka, S. Edenharter, L. Beaurenaut, “Lifetime modeling and simulation of power modules for hybrid electrical/electrical vehicles”, Volume 54, Issues 9–10, 2014, pages 1806-1812, Science Direct, London, ISSN 0026-2714, https://doi.org/10.1016/j.microrel.2014.07.009, 2014

[7] DIN e.V., DIN EN IEC 62196-1:2022, german version: Stecker, Steckdosen, Fahrzeugkupplungen und Fahrzeugstecker - Konduktives Laden von Elektrofahrzeugen - Teil 1: Allgemeine Anforderungen, Berlin, Germany 2022

[8] M. Vidmar, Lectures on the scientific fundamentals of electrical engineering, University Ljubljana, Slowenien, Print ISBN 978-3-642-52572-8, 1928

[9] C. Gerthsen, D. Meschede, Gerthsen Physik, Die ganze Physik zum 21. Jahrhundert, Springer, Berlin, ISBN 978-3-540-02622-8, 2004

[10] ZVEI, Zentralverband Elektrotechnik- und Elektroindustrie, Technischer Leitfaden Thermosimulationsmodelle Version 1.1, Köln, Germany 2020

[11] J.P. Huang, Transformation Thermotics for Thermal Conduction, Convection and Radiation, Springer, Singapore, Online ISBN 978-981-15-2301-4, January 2020

[12] C. Borgnakke, R. E. Sonntag, Fundamentals of Thermodynamics, Weinheim, Wiley, 10th Edition, ISBN: 978-1-119-72365-3, July 2020

[13] P. Steinmetz, Thermische Simulation einer CCS (Combined Charging System) Ladedose für Schwerlastkraftwagen, Hochschule Bonn-Rhein-Sieg, unpublished, April 2024